Journal of Theoretical Biology 466 (2019) 11–23

Contents lists available at ScienceDirect

Journal of Theoretical Biology

journal homepage: www.elsevier.com/locate/jtb

A mathematical model of the use of supplemental oxygen to combat surgical site infection

Chathranee Jayathilake[a], Philip K. Maini[b], Harriet W. Hopf[c], D.L. Sean McElwain[d], Helen M. Byrne[b], Mark B. Flegg[e], Jennifer A. Flegg[f,*]

[a] Department of Mathematics, Faculty of Science, University of Peradeniya, Sri Lanka
[b] Wolfson Centre for Mathematical Biology, Mathematical Institute, University of Oxford, Oxford, United Kingdom
[c] University of Utah, Utah, United States of America
[d] School of Mathematical Sciences and Institute of Health and Biomedical Innovation, Queensland University of Technology, Brisbane, Australia
[e] School of Mathematical Sciences, Monash University, Australia
[f] School of Mathematics and Statistics, University of Melbourne, Australia

ARTICLE INFO

Article history:
Received 4 June 2018
Revised 13 December 2018
Accepted 11 January 2019
Available online 16 January 2019

Keywords:
Numerical simulation
Partial differential equations
Surgical site infections
Wound healing

ABSTRACT

Infections are a common complication of any surgery, often requiring a recovery period in hospital. Supplemental oxygen therapy administered during and immediately after surgery is thought to enhance the immune response to bacterial contamination. However, aerobic bacteria thrive in oxygen-rich environments, and so it is unclear whether oxygen has a net positive effect on recovery. Here, we develop a mathematical model of post-surgery infection to investigate the efficacy of supplemental oxygen therapy on surgical-site infections.

A 4-species, coupled, set of non-linear partial differential equations that describes the space-time dependence of neutrophils, bacteria, chemoattractant and oxygen is developed and analysed to determine its underlying properties. Through numerical solutions, we quantify the efficacy of different supplemental oxygen regimes on the treatment of surgical site infections in wounds of different initial bacterial load. A sensitivity analysis is performed to investigate the robustness of the predictions to changes in the model parameters. The numerical results are in good agreement with analyses of the associated well-mixed model. Our model findings provide insight into how the nature of the contaminant and its initial density influence bacterial infection dynamics in the surgical wound.

1. Introduction

Infections are a common complication of any surgical procedure. The rate of infection varies depending on the procedure but can be as high as 10% for large bowel surgery (Health Protection Agency (HPA), 2012). Infection at the site of surgery lengthens a patient's hospital stay and is a risk factor for mortality (Astagneau et al., 2001; Coello et al., 2005). Furthermore, surgical site infections (SSIs) place considerable financial burden on healthcare providers. Indeed, each year SSIs cost the US healthcare system an estimated $3.3 billion (Zimlichman et al., 2013). For these reasons, it is important to understand how SSIs arise and to investigate approaches to reduce their incidence.

Several approaches are thought to reduce the risk of infection after surgery, including preventing perioperative hypothermia, managing blood glucose levels, and prescribing prophylactic antibiotics. Supplemental oxygen applied during and immediately after surgery is believed to increase the rate at which neutrophils (inflammatory cells) kill bacteria and, hence, reduce the risk of infection (Greif et al., 2000). Such a mechanism is supported by in vitro experiments; in 1976, Hohn demonstrated that the destruction of the bacterial species *S. aureus* by neutrophils increases with oxygen partial pressure (Hohn et al., 1976). Furthermore, the production of reactive oxygen species by neutrophils, which is crucial to immune function, was later shown to be limited by oxygen availability typically found in surgical wounds (Allen et al., 1997).

Despite these findings, clinical results of supplemental oxygen as a preventative measure for SSI are conflicting. Several groups report a reduced infection risk, while others report no signifi-

* Corresponding author.
E-mail addresses: chathraneej@pdn.ac.lk (C. Jayathilake), maini@maths.ox.ac.uk (P.K. Maini), harriet.hopf@hsc.utah.edu (H.W. Hopf), s.mcelwain@qut.edu.au (D.L. Sean McElwain), byrne@maths.ox.ac.uk (H.M. Byrne), mark.Flegg@monash.edu.au (M.B. Flegg), jennifer.flegg@unimelb.edu.au (J.A. Flegg).

https://doi.org/10.1016/j.jtbi.2019.01.021
0022-5193/

cant benefit (Belda et al., 2005; Gardella et al., 2008; Greif et al., 2000; Mayzler et al., 2005). Inconsistent conclusions also arose from three meta-analyses (Myles and Kurz, 2017; Qadan et al., 2009; Togioka et al., 2012). There are several possible explanations for the conflicting outcomes. Firstly, inter-patient variability was considerable, with patients undergoing different types of surgery. Secondly, SSIs are caused by a variety of bacterial species with different responses to oxygen. *S. aureus* is the most common SSI pathogen (Humphreys et al., 2016). It is an aerobic bacteria — it thrives in an oxygen rich environment. Finally, studies have employed different perioperative anesthetic management and associated fluid administration, which effects blood volume. Hypovolemia (decreased blood volume) limits the amount of oxygen delivered to the wound and would alter the effectiveness of oxygen treatments (Gottrup et al., 1987).

Under treatment with supplemental oxygen, there are competing effects between increased neutrophil destruction of bacteria and increased bacterial reproduction (in the case of *S. aureus*). Mathematical modelling has the potential to reveal how interactions between these two factors affect the response of an SSI to supplemental oxygen.

Existing mathematical models have been used to investigate the role of oxygen in healing, but typically without an infection present. Early work by Pettet et al. used partial differential equations (PDEs) to describe blood vessel growth into a wound in a reaction-diffusion-advection model. The role of oxygen was included implicitly, the vessel density serving as a proxy for oxygen levels to determine the motion of capillary tips (Pettet et al., 1996). Since then, similar continuum models of angiogenesis have been proposed that explicitly account for the oxygen concentration and its effect on the influx of immune cells. The focus has been on the role of immune cells like macrophages in promoting healing, rather than fighting infection (Maggelakis, 2003; Schugart et al., 2008; Vermolen and Adam, 2007). Meanwhile, others have investigated the potential therapeutic effects of oxygen. By modelling the impact of hyperbaric oxygen on chronic wounds and performing a parameter sensitivity analysis, they identifed parameter ranges for specific patient groups who may benefit from such treatment (Flegg et al., 2012; 2009).

Conversely, there exist mathematical models of infection which do not consider the effect of oxygen levels. For example, in the 1980s, Lauffenburger and colleagues developed several influential PDE models of infection, which incorporate bacteria, neutrophils and a non-specific neutrophil chemoattractant produced proportional to the extent of infection (Alt and Lauffenburger, 1987; Lauffenburger and Kennedy, 1983). Using scaling arguments and perturbation analysis, they derived a reduced system of ordinary differential equations (ODEs) describing the evolution of the total neutrophil and bacterial load across the domain. The ODE system was shown to admit multiple steady states, depending on the parameter values, including a persistent infection steady state and an elimination steady state. Since then, attention has focussed on ODE models under the spatially well-mixed assumption which incorporate more biological detail by, for example, distinguishing between different immune cell species or linking sets of equations from several pre-existing models (Dronne et al., 2004; Rudnev and Romanyukha, 1995). The aim of such models is usually to investigate how infections develop, although Vodovotz and colleagues have also produced a large body of work on the control of immune responses (Day et al., 2006; Mi et al., 2007; Reynolds et al., 2006). The infection model proposed by Smith *et al.* was notable for considering a specific bacterium, *S. Aureus*, rather than a generic one (Smith et al., 2011). Their model yielded two qualitatively different behaviours: bacterial elimination or sustained bacterial growth, depending on the initial amount of bacterial contamination. To the best of our knowledge, there are no published mathematical models of wound healing that explicitly include both infection and oxygen.

We develop a new mathematical model to study the ability of oxygen to prevent the development of an *S. aureus* bacterial infection within surgical wounds. We extend the model of Alt and Lauffenburger (Alt and Lauffenburger, 1987), which focussed on interactions between bacteria, neutrophils and a neutrophil chemoattractant, to include the important effect of oxygen on bacteria removal and reproduction. Whereas Alt and Lauffenburger reduced their PDE model to a system of simpler ODEs and performed analysis on that reduced system, we focus on the spatio-temporal changes that occur. We use diffusion terms to model cell migration and we employ nonlinear motility coefficients to prevent physically unrealistic model solutions that arise when using constant coefficients to model random motion (e.g. noncompact support).

Other ways in which our model differs from that of Alt and Lauffenburger (Alt and Lauffenburger, 1987) include the use of an excised surgical wound domain and the inclusion of surrounding healthy tissue with its important role in supplying oxygen and neutrophils to the wound. We also consider the treatment of surgical infections with supplemental oxygen in order to identify parameter regimes under which supplementary oxygen is beneficial to preventing the development of an infection. In our mathematical model, we do not consider the administration of prophylactic antibiotics that can be given to patients undergoing surgery (Hawn et al., 2013).

The remainder of this paper is structured as follows. In the Mathematical Model section, the PDE model of surgical wound infection is introduced and parameter values from the literature are summarised. We also investigate the relationship between model parameters and fundamental balances between bacterial growth and removal at a given oxygen level under a well-mixed assumption for bacteria. In the Results section, we present typical numerical solution profiles for the four model variables and also present results in which we vary key parameters, such as the initial bacterial load, the rate of bacterial killing by neutrophils and the treatment regime. In the Discussion, we draw conclusions on the success of supplemental oxygen therapy to treat surgical site infections and suggest model extensions.

2. Mathematical model

In this section, a dimensional mathematical model is developed for the interaction between the following species in an SSI in a one-dimensional (1D) domain:

- neutrophil density (cells/cm), denoted by $n(x, t)$
- *S. Aureus* bacteria density (cells/cm), denoted by $b(x, t)$
- chemoattractant concentration (ng/cm), denoted by $c(x, t)$
- oxygen concentration (mmHg), denoted by $w(x, t)$

where x is space and t is time. The role of each species in the model is described in the next subsection. The spatial scale of interest is a section of tissue, Ω, that is the union of a surgical wound on domain Ω_{wound}, surrounded by healthy tissue on domain $\Omega_{healthy}$ so that $\Omega = \Omega_{wound} \cup \Omega_{healthy}$ (see Fig. 1 for the ID domain that is adopted). More complicated wound geometries in higher dimensions could be considered, but here we adopt a 1D domain for simplicity. We take the length of the wound domain to be 0.3cm and the surrounding healthy tissue to have length 1cm, but a sensitivity analysis is performed on these values. We distinguish between the healthy and wounded domains. The healthy tissue is the source of neutrophils and oxygen and is also involved in the removal of the chemoattractant. A surgical wound infection will become clinically apparent around 5–7 days post surgery (Gelape, 2007) while granular tissue formation, epithelisation and angiogenesis will place take within several weeks

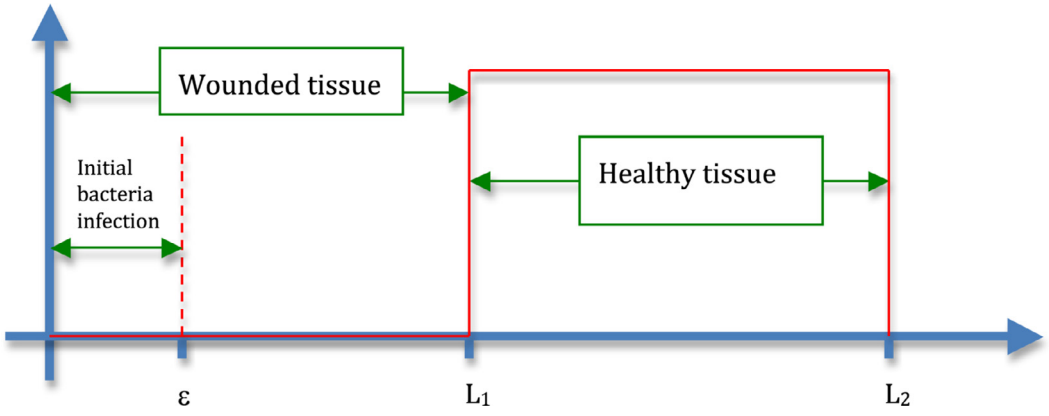

Fig. 1. A schematic of the 1D domain. The initial infection lies within $0 \le x \le \varepsilon$, the wounded domain on $0 \le x \le L_1$ (Ω_{wound}) and the surrounding healthy tissue on $L_1 < x \le L_2$ ($\Omega_{healthy}$).

(Enoch et al., 2006). The timescale of interest is therefore taken to be 10 days post surgery, long enough to know whether an infection has been prevented but not long enough for tissue repair to occur, so that we may assume that the boundary between the two domains does not move over time. Additionally, we do not consider the development of new blood vessels on this timescale. A continuum approach is adopted and PDEs are used to model the temporal and spatial evolution of the dependent variables listed above.

2.1. Governing equations

Neutrophils are assumed to move by nonlinear random motion and chemotaxis towards higher concentrations of the chemoattractant, c. Many chemical signals are involved in directing neutrophil movement, including interleukin-8 (IL-8) (Singer and Sansonetti, 2004), platelet derived growth factor (PDGF) (Enoch et al., 2006) and granulocyte-macrophage colony-stimulating factor (GM-CSF) (Shen et al., 2006). Since bacteria and neutrophil cells occupy a significant volume in the tissue compared to the other species in the model, we model their random motion with a nonlinear diffusion term. This also ensures compact support, which is biologically realistic for cells undergoing transport. Here we adopt the simplest approach and consider that the diffusion coefficients for n and b depend on themselves only but we note that other possibilities exist. Unless otherwise stated, we assume that model parameters are the same in the wounded and healthy tissue. For example, the diffusion coefficients for n and b could depend on both n and b; an approach adopted in Sherratt and Chaplain (2001). Neutrophils are also assumed to die at a constant rate λ_1 and are supplied to healthy tissue at rate λ_2. Combining these effects, we deduce that the following equation governs the evolution of the neutrophil density:

$$\frac{\partial n}{\partial t} = \underbrace{D_n \frac{\partial}{\partial x}\left(n \frac{\partial n}{\partial x}\right)}_{\text{random motion}} - \underbrace{\chi_n \frac{\partial}{\partial x}\left(n \frac{\partial c}{\partial x}\right)}_{\text{chemotaxis}} - \underbrace{\lambda_1 n}_{\text{death}} + \underbrace{\lambda_2 H(x \in \Omega_{healthy})}_{\text{supply from healthy tissue}}. \tag{1}$$

In Eq. (1), the positive constants D_n and χ_n represent the diffusion and chemotactic coefficients of the neutrophils, respectively. Furthermore, $H(x \in \Omega_{healthy})$ is the Heaviside function, which takes the value 1 in the healthy tissue region and 0 elsewhere.

Random movement of *S. Aureus* bacteria is modelled using a nonlinear random motion term, with diffusion constant D_b. Bacterial reproduction is modelled by a logistic term, with carrying capacity K_b and growth rate $f_1(w)$. Bacteria are killed by neutrophils at rate $f_2(w)$. Both rates $f_1(w)$ and $f_2(w)$ are regulated by the local oxygen concentration. Combining the above assumptions, the bacteria density is governed by the following equation:

$$\frac{\partial b}{\partial t} = \underbrace{D_b \frac{\partial}{\partial x}\left(b \frac{\partial b}{\partial x}\right)}_{\text{random motion}} + \underbrace{f_1(w) b \left(1 - \frac{b}{K_b}\right)}_{\text{logistic growth}} - \underbrace{\frac{f_2(w) n b}{b + B_1}}_{\text{neutrophil removal}}, \tag{2}$$

where B_1 is the density of bacteria that gives half-maximal killing of bacteria by neutrophils. We note that the carrying capacity of bacteria, K_b, may depend on the local oxygen concentration, but we ignore this possibility in order to keep the model as simple as possible while capturing the key features of an SSI.

For the rates $f_1(w)$ and $f_2(w)$, the following increasing, saturating functions of oxygen are proposed:

$$f_1(w) = \frac{f_{1Max} w}{w + W_1}, \quad f_2(w) = \frac{f_{2Max} w}{w + W_2},$$

where W_1 and W_2 are the oxygen concentrations that elicit half-maximal growth and killing rates, respectively.

The dominant processes affecting the evolution of the chemoattractant, c, are assumed to be diffusion, production, natural decay, and removal via the vasculature in the healthy tissue (note that we do not explicitly model the vasculature). We use linear terms to model the diffusion of the chemicals in the model (c and w) since their associated molecules do not occupy significant volume. It is assumed that the rate of production of chemoattractant increases with bacterial density, up to a maximum of λ_3 and that a bacteria level of B_2 stimulates half-maximal production. Chemoattractant is assumed to decay at rate λ_4 and is removed in the healthy tissue at rate λ_5. Combining these effects gives the following evolution equation for the chemoattractant concentration:

$$\frac{\partial c}{\partial t} = \underbrace{D_c \frac{\partial^2 c}{\partial x^2}}_{\text{diffusion}} + \underbrace{\frac{\lambda_3 b}{b + B_2}}_{\text{production}} - \underbrace{\lambda_4 c}_{\text{natural decay}} - \underbrace{\lambda_5 c H(x \in \Omega_{healthy})}_{\text{removal from healthy tissue}}. \tag{3}$$

It is assumed that oxygen is transported by diffusion and undergoes uptake by tissue at rate λ_6. Oxygen is consumed at rate λ_7 by bacteria and at rate λ_8 by neutrophils. The healthy tissue supplies oxygen at rate λ_9. The oxygen concentration is therefore governed by:

$$\frac{\partial w}{\partial t} = \underbrace{D_w \frac{\partial^2 w}{\partial x^2}}_{\text{diffusion}} - \underbrace{\lambda_6 w}_{\text{uptake by tissue}} - \underbrace{\lambda_7 w b}_{\text{bacteria uptake}} - \underbrace{\lambda_8 w n}_{\text{neutrophil uptake}} + \underbrace{\lambda_9 H(x \in \Omega_{healthy})}_{\text{supply to healthy tissue}}. \tag{4}$$

2.2. Geometry

For simplicity we focus on a 1D Cartesian geometry in which the surgical wound domain ($\Omega_{wound} \equiv 0 \le x \le L_1$) is surrounded by healthy tissue ($\Omega_{healthy} \equiv L_1 < x \le L_2$) as shown in Fig. 1. Here x measures the distance from the centre of the wound, parallel to the surface of the injured tissue. We take the domain to be symmetric about the centre of the wound, $x = 0$.

2.3. Boundary and initial conditions

Here $t = 0$ is taken to be the time immediately after surgery is finished. The entire domain ($0 \le x \le L_2$) is initially devoid of chemoattractant while an initial bacteria contamination of density b_{init} cells/cm is placed within $0 \le x \le \varepsilon$. In the results section we vary the location of the initial infection to investigate its ability to colonise the wound, all other things being equal. There are initially no neutrophils and oxygen within the wounded domain ($0 \le x \le L_1$), while neutrophils and oxygen take their healthy tissue values of n_0 and $\overline{w}$, respectively, in the healthy tissue region ($L_1 < x \le L_2$). Hence, we have the following initial conditions:

$$c(x,0) = 0, \quad 0 \le x \le L_2; \qquad b(x,0) = \begin{cases} b_{init} & 0 \le x \le \varepsilon, \\ 0 & \varepsilon < x \le L_2; \end{cases}$$

$$n(x,0) = \begin{cases} 0 & 0 \le x \le L_1, \\ n_0 & L_1 < x \le L_2; \end{cases} \qquad w(x,0) = \begin{cases} 0 & 0 \le x \le L_1, \\ \overline{w} & = L_1 < x \le L_2. \end{cases} \tag{5}$$

No flux boundary conditions are prescribed at the wound centre ($x = 0$) due to symmetry and at the outer boundary of the domain ($x = L_2$) since the outer boundary is considered far away from the wound interface:

$$n\frac{\partial n}{\partial x} = b\frac{\partial b}{\partial x} = \frac{\partial c}{\partial x} = \frac{\partial w}{\partial x} = 0 \quad \text{at} \quad x = 0 \quad \text{and} \quad x = L_2. \tag{6}$$

2.4. Analysis of a reduced model: Bacteria versus neutrophils

In Section 3, we present a numerical investigation into the behaviour of the PDE model (Eqs. (1)–(4)). In order to interpret some key features of this spatio-temporal model, in this section we make model simplifications and proceed to analyse a reduced model. The simplification involves ignoring the transport term for bacteria. Whilst this situation is unlikely to be realised *in vivo*, we find that investigating the properties of the reduced model gives considerable insight into the interface in parameter space which separates regions of bacteria domination and bacteria elimination that are not easily accessible with simulations alone.

Since the fate of the bacteria is regulated by oxygen levels, our first step is to consider a characteristic level of oxygen, $w = w_0$. One approach would be to take a constant value w_0. An alternative is to approximate the spatially varying oxygen profile, $w_0 = w_0(x)$; we provide an example in the Appendix. In the analysis that follows, we assume that the characteristic level of oxygen, w_0, has been determined.

We consider the behaviour of the bacterial density, under the mathematical condition of being well-mixed. That is, we neglect the random motion of bacteria and consider that the bacterial density satisfies the following ordinary differential equation (ODE):

$$\begin{aligned} \frac{\mathrm{d}b}{\mathrm{d}t} &= \frac{f_{1Max}w_0}{(w_0+W_1)} b\left(1 - \frac{b}{K_b}\right) - \frac{f_{2Max}w_0}{(w_0+W_2)}\frac{nb}{(b+B_1)} \\ &= g(b, w_0) - p(b, w_0, n), \end{aligned} \tag{7}$$

where we denote the growth term by $g(b, w_0)$ and the phagocytosis (removal) term by $p(b, w_0, n)$. On a microscopic scale, bacteria will undergo random motion, however on the macroscopic scale bacterial colonies have been observed to stay in microcolony structures to resist host defenses, so that neglecting "diffusion" on a macroscopic scale is not unreasonable as a first order approximation (Davis et al., 2015).

In Eq. (7), the phagocytosis term will not effect the bacterial density until the neutrophils reach the bacteria, since $p(b, w_0, 0) = 0$. That is, the bacteria will undergo logistic growth until the arrival of neutrophils at the site of the infection. Let us denote the time that it takes for the neutrophils to reach the bacteria as τ. In the healthy tissue, the neutrophils can be approximated by $n \sim \frac{\lambda_2}{\lambda_1} = n_0$ since the chemoattractant gradient will be negligible in this region. We assume that this healthy concentration of neutrophils is transported via chemotaxis into the wound to reach the location of the bacteria:

$$n(x,t) \sim n_0 H(x - x_0(t)), \tag{8}$$

where $x_0(t)$ is the location of the front of the neutrophils which will depend on the chemoattractant profile. Here, we do not consider the exact value of τ when the neutrophils arrive at the site of bacteria infection, we only consider that this time can be quantified and that the neutrophil density at that time is approximated by $n \sim n_0$.

Hence, the bacterial density (at each point in the domain) is governed by

$$\frac{\mathrm{d}b}{\mathrm{d}t} = \begin{cases} \dfrac{f_{1Max}w_0}{(w_0+W_1)} b\left(1 - \dfrac{b}{K_b}\right) & 0 \le t \le \tau, \\ \dfrac{f_{1Max}w_0}{(w_0+W_1)} b\left(1 - \dfrac{b}{K_b}\right) - \dfrac{f_{2Max}w_0}{(w_0+W_2)}\dfrac{n_0 b}{(b+B_1)} & \tau < t \end{cases} \tag{9}$$

subject to $b(0) = b_{init}$ (assuming we are in a region of initial bacterial infection, otherwise the trivial solution holds, $b(t) = 0$).

The solution at time $t = \tau$ is given by

$$b(\tau) = \frac{b_{init}K_b}{(K_b - b_{init})\exp(-f_{1Max}w_0\tau/(w_0+W_1)) + b_{init}}, \tag{10}$$

where Eq. (10) is the solution of the logistic equation at $t = \tau$. For small τ and b_{init}, we have:

$$b(\tau) \approx b_{init}\exp\left(\frac{f_{1Max}w_0\tau}{(w_0+W_1)}\right), \tag{11}$$

which solves the linearised ODE in Eq. (9) for early times.

For $t > \tau$, we solve

$$\frac{\mathrm{d}b}{\mathrm{d}t} = \frac{f_{1Max}w_0}{(w_0+W_1)} b\left(1 - \frac{b}{K_b}\right) - \frac{f_{2Max}w_0}{(w_0+W_2)}\frac{n_0 b}{(b+B_1)} = g(b) - p(b), \tag{12}$$

subject to $b(\tau) = b_{init}\exp\left(\frac{f_{1Max}w_0\tau}{(w_0+W_1)}\right)$.

The long-term behaviour of Eq. (12) can be determined by considering the stability of its steady states. The possible steady states are

$$b = 0, \quad \text{and} \quad b_{\pm} = \frac{K_b - B_1}{2} \pm \sqrt{\left(\frac{K_b + B_1}{2}\right)^2 - \Phi}. \tag{13}$$

where $\Phi = \frac{K_b n_0 f_{2Max}(w_0+W_1)}{f_{1Max}(w_0+W_2)}$ is a dimensionless measure of f_{2Max} holding the other parameters (K_b, n_0, w_0, W_1, f_{1Max} and W_2) constant. The value of Φ determines the number of positive steady states; zero, one or two as summarised below.

1. *Regime 0: clearance of bacteria, no positive steady states*

   When $\Phi > \left(\frac{K_b+B_1}{2}\right)^2$, we find that $p(b) > g(b)$ for all $b > 0$ (since all parameters in Eq. (12) are positive constants) and hence there are no positive steady states (see intersection of red curve

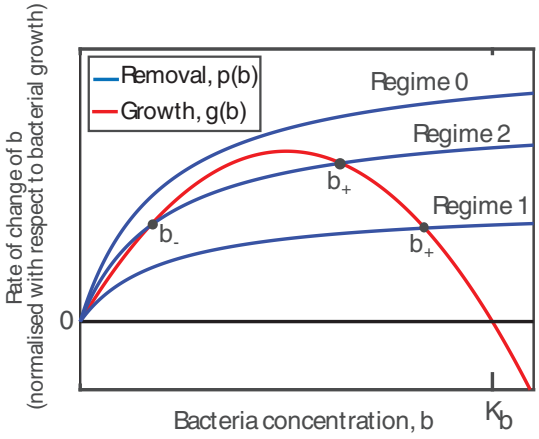

Fig. 2. Schematic indicating the three different regimes in the well-mixed approximation. The red line represents bacteria growth as a function of the bacteria density, $g(b)$, in Eq. (12), while the blue curves represent three different regimes of bacteria death, $p(b)$. The three regimes of bacteria removal (by varying Φ) lead to zero, one and two positive steady states, respectively. The steady states of the well-mixed model are given by the intersection of the different coloured curves. The vertical scale is normalised with respect to the factor $f_{1Max}w_0/(w_0+W_1)$. (For interpretation of the references to colour in this figure legend, the reader is referred to the web version of this article.)

and blue curve denoted by 'Regime 0′ in Fig. 2). That is, $b=0$ is an asymptotically stable steady state and, hence, in this regime, neutrophils dominate the dynamics until the bacteria is cleared (even for the most severe infection).

2. *Regime 1: bacterial persistence, one positive steady state*
When $\Phi < K_b B_1$, there is one positive steady state $b=b_+$. Since $g(b)>p(b)$ for $0<b<b_+$ and $p(b)>g(b)$ for $b>b_+$ it follows that $b=b_+$ is an asymptotically stable steady state and $b=0$ is unstable (Fig. 2, 'Regime 1′). Hence, in this parameter regime, we conclude that bacterial infection will not be cleared (irrespective of its severity).
3. *Regime 2: bacterial elimination or persistence, two positive steady states*
When $K_b B_1 \le \Phi \le \left(\frac{K_b+B_1}{2}\right)^2$, there are two positive steady states, $b=b_-$ and $b=b_+$, where $0<b_-<b_+$. By similar arguments as above, $b=0$ and $b=b_+$ are both asymptotically stable but $b=b_-$ is unstable (Fig. 2, 'Regime 2′). In this regime, if the system is initiated (at time $t=\tau$) with $b<b_-$, the bacterial infection will be cleared but if $b>b_-$, we expect the bacterial infection to approach the steady state b_+. That is, b_- is a point of bifurcation; when seeded with $b>b_-$ the bacteria persist and when $b<b_-$ they are eliminated. Hence, $[0, b_-)$ is the basin of attraction for the elimination steady state and (b_-, ∞) is the basin of attraction for long-term persistence of bacteria. The outcome of the infection therefore depends on the severity of the initial infection, the rate of bacterial growth as well as the killing efficiency of neutrophils entering the wound (by reducing the bacterial population and not letting it grow out of control).

Regime 2 is the only situation where the severity of the initial infection determines the long-term outcome; eventual bacterial clearance or bacterial persistence. The switching of this behaviour occurs when the point of bifurcation, b_-, is equal to the density of bacteria when the neutrophils arrive, $b(\tau)$. In the (f_{2Max}, b_{init}) parameter space, the locus formed by the bifurcation point determines an interface between regions of bacterial elimination and bacterial persistence. Putting Eq. (11) into b_- in Eq. (13), we get:

$$b_{init} - b_0 = -\gamma\sqrt{f_0 - f_{2Max}}, \tag{14a}$$

where

$$b_0 = \frac{K_b - B_1}{2}\exp\left(\frac{-f_{1Max}w_0\tau}{(w_0+W_1)}\right), \tag{14b}$$

$$\gamma = \exp\left(\frac{-f_{1Max}w_0\tau}{(w_0+W_1)}\right)\sqrt{\frac{K_b n_0(w_0+W_1)}{f_{1Max}(w_0+W_2)}}, \tag{14c}$$

and

$$f_0 = \left(\frac{K_b+B_1}{2}\right)^2\frac{f_{1Max}(w_0+W_2)}{K_b n_0(w_0+W_1)}. \tag{14d}$$

The shape of the interface is characterised in Fig. 3 as b_{init} and f_{2Max} vary and is in good agreement with the shape of the interface obtained from numerical results for the full PDE model (Figs. 7 and 8). The analysis suggests that the bacteria are either cleared or the wound suffers an ongoing bacterial load. As the supply of neutrophils (n_0) increases, Φ will also increase until a critical point in Regime 2, where the neutrophil killing rate is such that they clear the bacteria entirely (solid blue line in Fig. 3). The analysis also provides insight into the effect of supplemental oxygen, since $\Phi = \frac{K_b n_0 f_{2Max}(w_0+W_1)}{f_{1Max}(w_0+W_2)}$ depends on the characteristic oxygen level, w_0. We see that Φ increases with increasing w_0 if $W_1<W_2$ but decreases if $W_2<W_1$. Increasing Φ by increasing w_0 in the case where $W_1<W_2$ shifts the regime boundaries (dashed black lines) in Fig. 3 to the left and therefore requires less from the neutrophil supply to clear the bacteria (e.g. f_{2Max} can decrease and still clear bacteria). Conversely, if $W_2<W_1$, increasing oxygen would mean that neutrophils need to kill bacteria more efficiently to clear the bacteria (e.g. f_{2Max} will need to be increased to still clear the infection). Hence, the success of supplemental oxygen therapy will be influenced by how the growth of bacteria and removal of bacteria depend on the oxygen concentration through the parameters W_1 (half-maximal bacteria growth rate) and W_2 (half-maximal removal rate). These parameters may be characteristic of a particular strain of bacteria and will likely vary between different strains.

2.5. Parameter estimates

The mathematical model outlined above (see Eqs. (1)–(4)) includes many parameters that can be estimated from the experimental literature. Table 1 lists parameter values and their associated sources for the 1D model. It should be noted that the experimental methods from which these estimates derive vary considerably. As such, these references are used as a guide only to identify reasonable parameter values. Additional details for certain parameters are given below:

- The random motility coefficient for neutrophils (D_n) was chosen so that the neutrophil-rich diffusion coefficient was 10 times less than the chemotaxis coefficient (χ_n). In this way, the motion of neutrophils is dominated by chemotaxis, as is typically observed in cell migration (Lauffenburger, 1983; Stokes and D.A., 1991). Hence, we take, $D_n = 0.1\chi_n/n_0$.
- The neutrophil supply rate, λ_2, was chosen so that, in the absence of spatial migration, balancing neutrophil decay and supply in the healthy tissue region gives a density of resident neutrophils typical of that found in healthy, undamaged tissue (where $n=n_0$). Hence, we take $\lambda_2 = \lambda_1 n_0$.
- Following the work of Wood et al. (2002), the effective diffusivity in a porous medium can be described by Maxwell's solution:
$$\frac{D_p}{D} = \frac{2(1-\alpha)}{2+\alpha},$$
where D is the diffusivity in the extracellular fluid, D_p is the effective diffusivity throughout the porous medium and α is

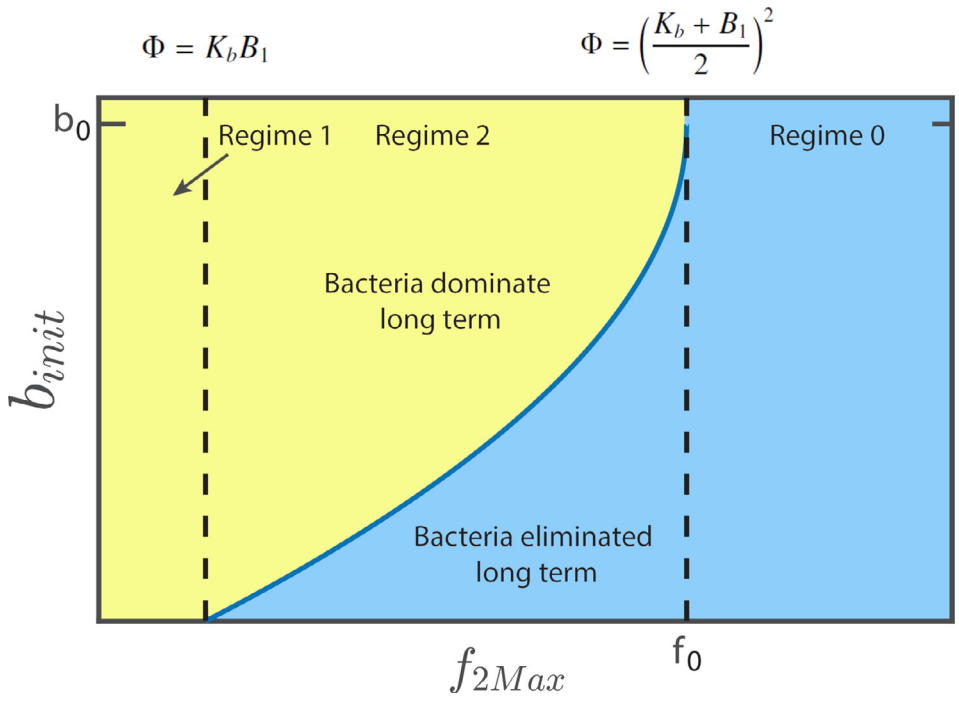

Fig. 3. Schematic showing how the long-term SSI outcome changes, as b_{init} and f_{2Max} vary, under the well-mixed assumption. Dominance of the infection (yellow) and successful clearance of the infection by neutrophils (blue) are shown. The boundaries between the regimes are shown in dashed black lines. Under parameter regime 0 ($\Phi > \left(\frac{K_b+B_1}{2}\right)^2$), only bacterial elimination is possible while under regime 1 ($\Phi < K_b B_1$) only bacterial dominance can occur. Under regime 2 ($K_b B_1 \le \Phi \le \left(\frac{K_b+B_1}{2}\right)^2$), both outcomes are possible. The interface in (f_{2Max}, b_{init}) parameter space where the outcome changes is given by Eq. (14a) and is shown here in the solid blue line. The interface under the well-mixed assumption shown here approximates well the interface seen in numerical simulations of the full PDE model (see Fig. 8). Recall that $\Phi = \frac{K_b n_0 f_{2Max}(w_0+W_1)}{f_{1Max}(w_0+W_2)}$, so when $f_{2Max} = f_0$ (see Eq. 14d), it follows that $\Phi = \left(\frac{K_b+B_1}{2}\right)^2$. (For interpretation of the references to colour in this figure legend, the reader is referred to the web version of this article.)

the volume fraction of extracellular material. Fixing $\alpha = 0.85$ (Stephen, 2013) and taking the random motility coefficient for bacteria in culture to be $D = 1.81\,\text{cm}^2/\text{day}$ for *S. Aureus* (Yeong-Chul, 1996), gives the diffusion coefficient (at maximal bacterial density) in the surgical wound as $D_b = 0.191/K_b\ \text{cm}^2/\text{day}$. Note that the factor K_b accounts for the nonlinear diffusion coefficient for bacteria; an equivalent value for a linear diffusion coefficient would be given by $D \sim D_b K_b$ when $b \approx K_b$. It should also be noted that this theory was developed to estimate the diffusivity of chemicals through cellular environments; we use it here as a guide to estimate the diffusion coefficient of bacteria in surgical wounds.

- The rate at which bacteria consume oxygen (λ_7) was taken to be 100 fold less than that at which neutrophils consume oxygen (λ_8); this estimate is based on the assumption that neutrophils consume oxygen at significantly greater rate than bacteria because of their larger cellular volume.
- The oxygen supply rate in healthy tissue, λ_9, was chosen so that in the absence of diffusion, the oxygen concentration in the healthy tissue region would be the oxygen tension in healthy tissue, $\overline{w}$. That is, $\lambda_9 = (\lambda_6 + \lambda_8 n_0)\bar{w}$, where estimates of λ_6, λ_8, n_0 and $\bar{w}$ are given in Table 1.
- Surgical wounds are generally created in a "sterile" environment, so that the wounds we consider typically have low levels of bacteria. We have therefore varied this parameter (b_{init}) over a range of values (per cm) that represent a small initial bacterial load, compared to the carrying capacity of the tissue. The baseline value is taken to be $b_{init} = 5000/\text{cm}$.
- Estimates of the rate of bacteria removal (f_{2Max}) are not directly available from the literature, to the best of our knowledge. We have therefore varied f_{2Max} to quantify differences in model outcome.

2.6. Numerical method

Eqs. (1)–(4) were solved for a 1D wound in a Cartesian geometry (Fig. 1), subject to the prescribed initial and boundary conditions (Eqs. (5) and (6), respectively). The numerical solution of the dimensional equations was obtained using MATLAB's `pdepe.m`, which approximates the solution to initial-boundary value problems for systems of parabolic and elliptic PDEs in one space variable and time (there must be at least one parabolic equation) (MathWorks, 2017). We compare the final bacterial load at $t_{final} =$ 10 days as the parameter values are varied. The bacterial load, B_{load}, at time t was defined to be:

$$B_{load}(t) = \int_{x=0}^{x=L_2} b(x,t)\,dx$$

and was approximated using the Trapezoidal rule.

2.7. Treatment regimes

To understand the effect of supplemental oxygen therapy on the final bacterial load, three regimes were simulated: no treatment, 30% oxygen for 2 h post surgery (control therapy) and treatment with 80% oxygen for 6 h post surgery (experimental treatment). These were implemented as follows:

- For no treatment, the arterial oxygen concentration was unchanged from the baseline value in Table 1 ($\bar{w} = 80$ mmHg), which represents the oxygen tension in healthy tissue under room conditions ($\sim$21% oxygen).
- For the control therapy of 30% oxygen for 2 h post surgery, the value of $\bar{w}$ was set to 121 mmHg for the first 2 h after surgery (and then returned to the baseline value, $\bar{w} = 80$ mmHg). This is consistent with the control treatment regimes in Qadan et al.,

Togioka et al. and Miles et al. (Myles and Kurz, 2017; Qadan et al., 2009; Togioka et al., 2012). We denote this as treatment A.

- For 80% oxygen for 6 h post surgery, the value of $\bar{w}$ was set to 348 mmHg for the first 6 h after surgery (and then returned to the baseline value, $\bar{w} = 80$ mmHg). This is consistent with the experimental treatment regimes in Qadan et al. (2009); Togioka et al. (2012) and Myles and Kurz (2017). We denote this as treatment B.

The change in $\bar{w}$ value affects the oxygen supply rate λ_9 (see Table 1). The values of $\bar{w}$ under treatment were taken from a study by Grief et al. in which the oxygen arterial partial pressure during surgery was 121 ± 34 mmHg in patients receiving 30% oxygen and 348 ± 97 mmHg in the 80% group (Greif et al., 2000).

Here we assume that the surrounding tissue is adequately perfused so that hypovolemia (decreased blood volume) does not effect the oxygen treatment.

3. Results

We use the mathematical model to simulate the time course of different surgical wound infections in response to different treatment regimes. With parameter values as per Table 1 and a neutrophil population which is extremely effective at removing bacteria ($f_{2Max} = 30$), the model predicts that the surgical site infection is removed by the neutrophils without any treatment. Fig. 4 shows the spatio-temporal behaviour of the four species (neutrophils, bacteria, chemoattractant and oxygen). The initial bacteria infection (on $0 \le x \le \varepsilon = 0.1$) elicits an immune response; the bacteria stimulate the release of chemoattractant which, in turn, attracts neutrophils to the site of infection. The neutrophils clear the infection so that the final bacterial load vanishes ($t_{final} = 10$ days). Also, at $t_{final} = 10$ days, there is negligible chemoattractant in the domain, while oxygen and neutrophils reach bacteria-free steady states in the healthy tissue. The oxygen concentration is close to zero inside the wound domain since there is no oxygen supply (oxygen supplied by the intact vasculature in the healthy tissue only) so that oxygen can enter the wound region only by diffusion and is quickly consumed by cells (see Eq. (4)). We note that while the amount of oxygen is low in the wound domain, this does not mean that the cells receive low oxygen; instead oxygen diffuses into the wound and is consumed, resulting in low oxygen levels. Since angiogenesis is neglected in this model, the interface between the healthy and wound tissues does not move and the oxygen is unable to diffuse any further into the wound space. Note that the validity of our results depends on the validity of assuming that the time scale of interest (10 days) is not long enough for tissue repair and/or angiogenesis to occur, so that the boundary between the two domains does not move over time. The level of oxygen outside the wounded tissue is elevated during the simulation at times when the oxygen-consuming neutrophils are depleted. The neutrophils are being attracted into the centre of the wound site to deal with the bacteria. After the bacteria are removed (at later times) neutrophils are no longer depleted outside the wound and oxygen levels there return to normal.

With the same parameters used to generate Fig. 4 and a less effective neutrophil population (f_{2Max} reduced from $f_{2Max} = 30$ to $f_{2Max} = 2$), the neutrophils are unable to clear the surgical site infection. Fig. 5 shows the spatio-temporal response of the four species to an initial bacteria infection (on $0 \le x \le \varepsilon = 0.1$). Again, the bacteria elicit an immune response resulting in neutrophil infiltration of the infection. In this case, however, the neutrophils fail to clear the infection which instead spreads over the entire domain and grows substantially (that is, $b(x, t_{final}) \gg b_{init}$ for all $x \in [0, L_2]$). The bacterial density is relatively low until $t = 4$ days, compared to the bacterial density at large times, which is approximately spatially uniform. The oxygen concentration is again low in the wound space, since oxygen is supplied only in the healthy tissue and the interface between healthy and wound tissue does not move over time. Oxygen that is supplied to the wound by diffusion is quickly consumed by the cells. On the other hand, there is high oxygen concentration just outside the wound, due to the migration of oxygen-consuming neutrophils from the healthy tissue into the wound space. The level of oxygen outside the wounded tissue is elevated throughout the simulation since the neutrophils have been depleted and remain so until the final time, $t_{final} = 10$ days. The bacteria distribution undergoes what appears to be a sudden shift from low bacteria concentrations (at small times) to large ones (at large times). This is characteristic of the logistic-type term used to model bacteria growth. (Eq. (2)), which is one well-accepted model for bacteria growth (Zwietering et al., 1990).

The results presented in Figs. 4 and 5 show that the mathematical model gives rise to (at least) two possible behaviours at long times:

- $b = 0$ everywhere (elimination), which we denote as state 0;
- $b \gg b_{init}$ everywhere (infection), which we denote as state 1.

These outcomes are consistent with the predictions of the well-mixed model outlined in Section 2.4 where we found at most two long-term outcomes: bacterial elimination or bacteria persistence. We now investigate this behaviour further by varying the initial bacterial load (b_{init}) and the maximum rate at which neutrophils kill bacteria (f_{2Max}) as per Fig. 3 under no treatment, the control treatment (treatment A) and the experimental treatment (treatment B).

Fig. 6 shows the final bacterial load (at $t_{final} = 10$ days) when b_{init} is varied from 5 to 50,000 and f_{2Max} is varied from 1 to 90 under no treatment. The bacteria are eliminated (dark blue zone) for combinations of low b_{init} values and high f_{2Max} values. For low f_{2Max} and high b_{init} values, there is a sustained bacterial infection (yellow zone). Fig. 7 shows the final bacterial load when b_{init} and f_{2Max} are varied while under treatment A (30% oxygen for 2 h), where the solid red line indicates the separation of the (f_{2Max}, b_{init}) parameter space in terms of bacterial elimination (state 0) and bacterial infection (state 1), under no treatment (Fig. 6). Again, regions of the parameter space in which bacteria are eliminated are shown in dark blue while regions in which there is a sustained bacterial infection are depicted in yellow. The mathematical model predicts that the control treatment may increase the risk of surgical site infection. That is, there are some regions of parameter space in which the bacteria are eliminated without treatment (Fig. 6) and which support an infection when the wound is treated with the control therapy (Fig. 7). The final size of the bacteria population, if the bacteria are allowed to flourish, is close to the carrying capacity of the tissue (see Table 1).

Fig. 8 shows the final bacterial load when b_{init} and f_{2Max} are varied under treatment B (80% oxygen for 6 h). The solid red and pink lines indicate the separation of the (f_{2Max}, b_{init}) parameter space in terms of bacterial elimination and bacterial infection under no treatment (Fig. 6) and the control therapy (Fig. 7), respectively. Under the mathematical model, the experimental treatment reduces the risk of surgical site infection compared to the control treatment, but the risk of infection is slightly increased compared to the case of no treatment. Comparing the solid pink line to the interface generated under treatment B, a shift to the left is observed. This behaviour is consistent with the analysis from Section 2.4 since in these simulations we have $W_1 < W_2$ (see also Fig. 3).

We performed a sensitivity analysis to investigate the effect of changes in the parameter values on the outcome of the surgical wound under no treatment, the control (treatment A) and experimental (treatment B) therapies. We changed each parameter by a

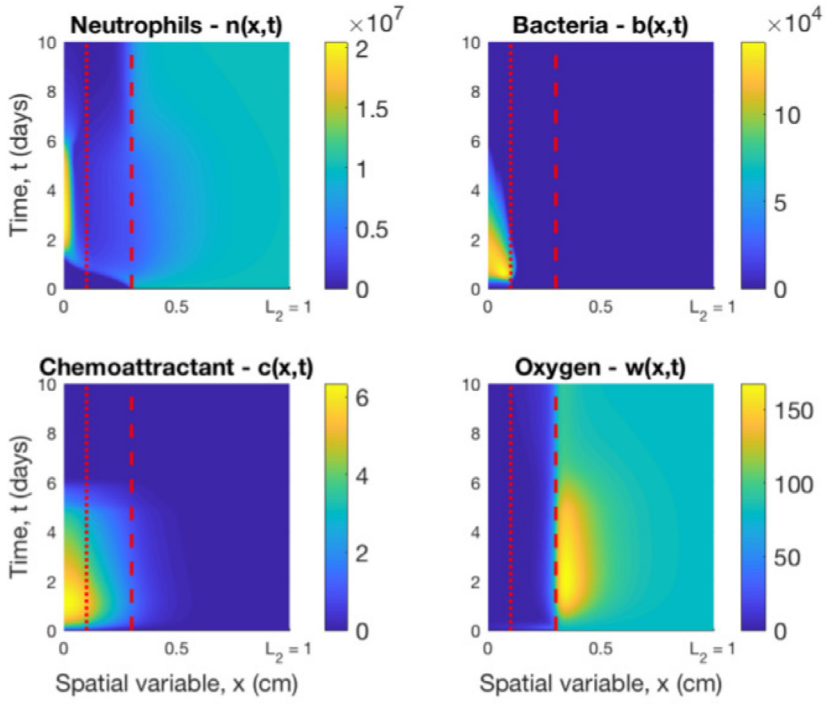

Fig. 4. Spatio-temporal behaviour of neutrophils, bacteria, chemoattractant and oxygen in surgical wound with $b_{init} = 5000$ and $f_{2Max} = 30$. All other parameter values are fixed as per Table 1. After 10 days, the bacteria have been eliminated from the surgical wound site. The red dotted line represents the location of ε (size of initial bacteria domain) and the red dashed line represents the location of L_1 (length of wounded tissue). (For interpretation of the references to colour in this figure legend, the reader is referred to the web version of this article.)

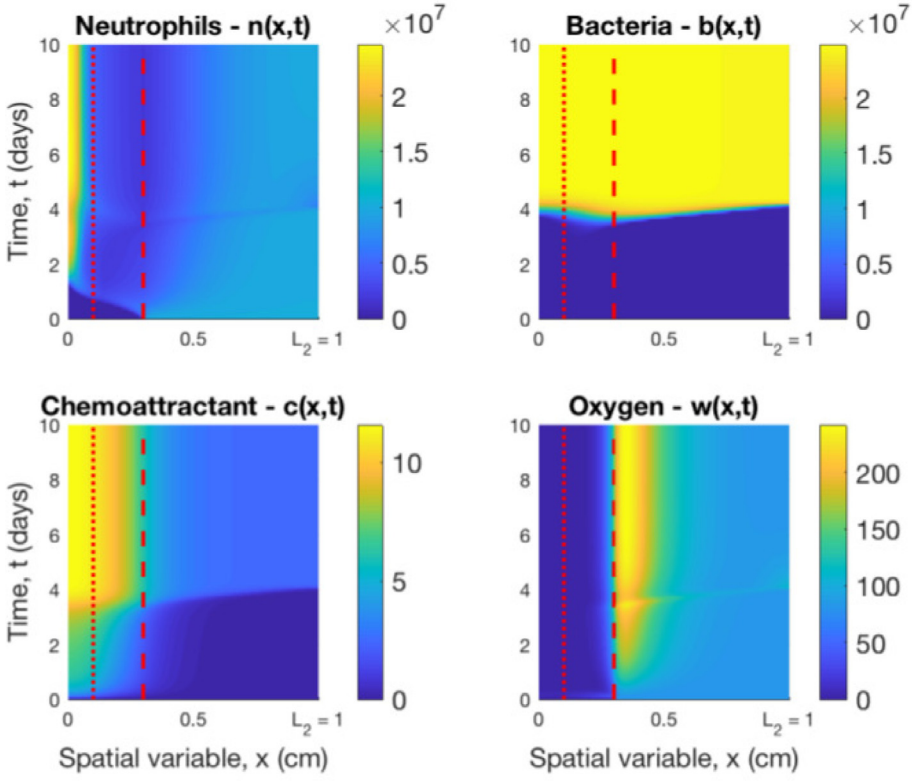

Fig. 5. Spatio-temporal behaviour of neutrophils, bacteria, chemoattractant and oxygen in surgical wound with $b_{init} = 5000$ and $f_{2Max} = 2$ (reduced from $f_{2Max} = 30$ in Fig. 4). All other parameter values as per Table 1. After 10 days, the bacterial infection has become established in the wound site. The red dotted line represents the location of ε (size of initial bacteria domain) and the red dashed line represents the location of L_1 (length of wounded tissue). (For interpretation of the references to colour in this figure legend, the reader is referred to the web version of this article.)

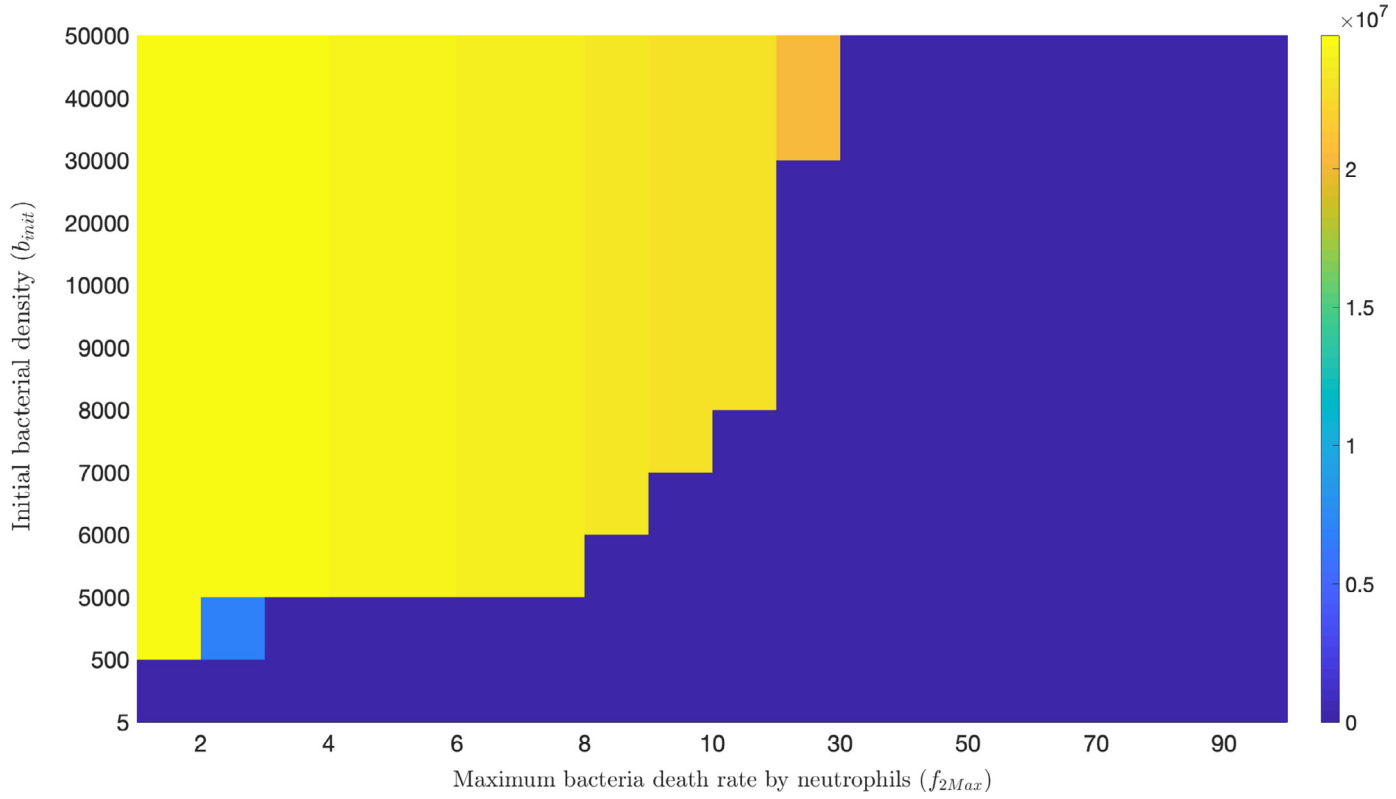

Fig. 6. Final bacterial density (at $t_{final} = 10$ days) without any treatment as b_{init} (initial bacterial density, vertical axis) and f_{2Max} (maximum bacteria death rate by neutrophils, horizontal axis) are varied. All other parameter values are fixed as per Table 1.

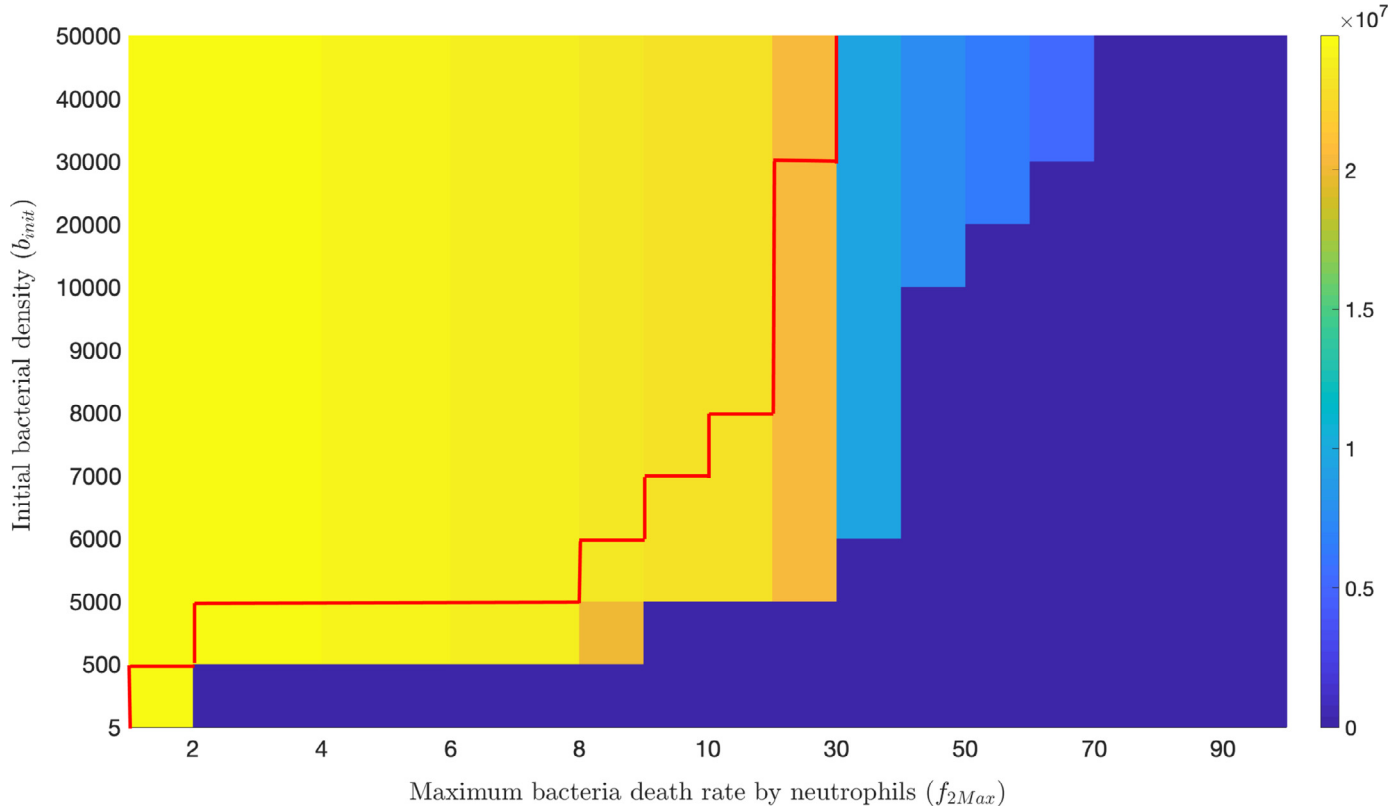

Fig. 7. Final bacterial density (at $t_{final} = 10$ days) with treatment A (30% oxygen for 2 h post surgery) as b_{init} (initial bacterial density, vertical axis) and f_{2Max} (maximum rate of bacterial killing by neutrophils, horizontal axis) are varied. All other parameter values are fixed as per Table 1. Surgical wounds with small initial bacterial density and/or high bacterial killing give rise to long-term bacterial elimination. For comparison, the solid red line represents the separation of the (f_{2Max}, b_{init}) parameter space in terms of bacteria elimination and bacteria infection, under no treatment (Fig. 6). (For interpretation of the references to colour in this figure legend, the reader is referred to the web version of this article.)

Table 1
Baseline parameter values for the 1D mathematical model, with supporting references ('TW' refers to this work). Where applicable, expressions used for parameter values are given in brackets in the second column. Additional details for some parameter values are given in the main text (Section 2.5).

Parameter	Interpretation	Dimensional value	Source
n_0	Neutrophil healthy tissue density	1×10^7 neutrophils/cm	Min-Ho et al. (2008)
$\overline{w}$	Arterial oxygen partial pressure	80 mmHg	Belda et al. (2005)
b_{init}	Initial bacterial density	5000 bacteria/cm	TW
D_n	Neutrophil diffusion coefficient ($0.1\chi_n/n_0$)	2×10^{-10} cm^3/day/neutrophil	TW
χ_n	Neutrophil chemotactic coefficient	0.02 cm^3/day/ng	Ebrahimzadeh et al. (2000); Jeon et al. (2002)
λ_1	Neutrophil death rate	log(2) /day	Cheretakis et al. (2006)
λ_2	Neutrophil supply rate ($\lambda_1 n_0$)	6.93×10^6 neutrophils/cm/day	TW
D_b	Bacterial diffusion coefficient ($0.191/K_b$)	7.64×10^{-9} cm^3/day/bacteria	TW, Yeong-Chul (1996)
K_b	Bacterial carrying capacity	2.5×10^7 bacteria/cm	Kim et al. (2008)
B_1	Bacteria that gives half-maximal killing	100 bacteria/cm	Romanyukha et al. (2006)
W_1	Oxygen that gives half-maximal bacteria growth	5 mmHg	TW
W_2	Oxygen that gives half-maximal bacteria killing	80 mmHg	TW
f_{1Max}	Maximum bacteria growth rate	18 /day	TW
f_{2Max}	Maximum rate that neutrophils can kill bacteria	30 bacteria/neutrophil/day	TW
D_c	Chemoattractant diffusion coefficient	0.216 cm^2/day	Moghe et al. (1995)
λ_3	Production rate of chemoattractant ($20\lambda_4$)	80log(2) /day	Iocono et al. (2000)
B_2	Bacteria that gives half-maximal chemoattractant production	500 bacteria/cm	TW
λ_4	Chemoattractant decay rate	4log(2) /day	Chung-Sheng et al. (2008); Laterveer et al. (1996)
λ_5	Chemoattractant removal rate	20 /day	TW
D_w	Oxygen diffusion coefficient	0.173 cm^2/day	Sasaki et al. (2012)
λ_6	Oxygen decay rate	15 /day	TW, Hunt and Hopf (1997)
λ_7	Oxygen consumption by bacteria	7×10^{-7}/day/(bacteria/cm)	TW
λ_8	Oxygen consumption by neutrophils	7×10^{-5} /day/(neutrophils/cm)	Allen et al. (1997)
λ_9	Oxygen supply rate ($(\lambda_6 + \lambda_8 n_0)\overline{w}$)	5.72×10^4 mmHg/day	TW
ε	Size of initial bacterial domain	0.1 cm	TW
L_1	Length of wounded tissue	0.3 cm	TW
L_2	Outer length (healthy tissue)	1.0 cm	TW

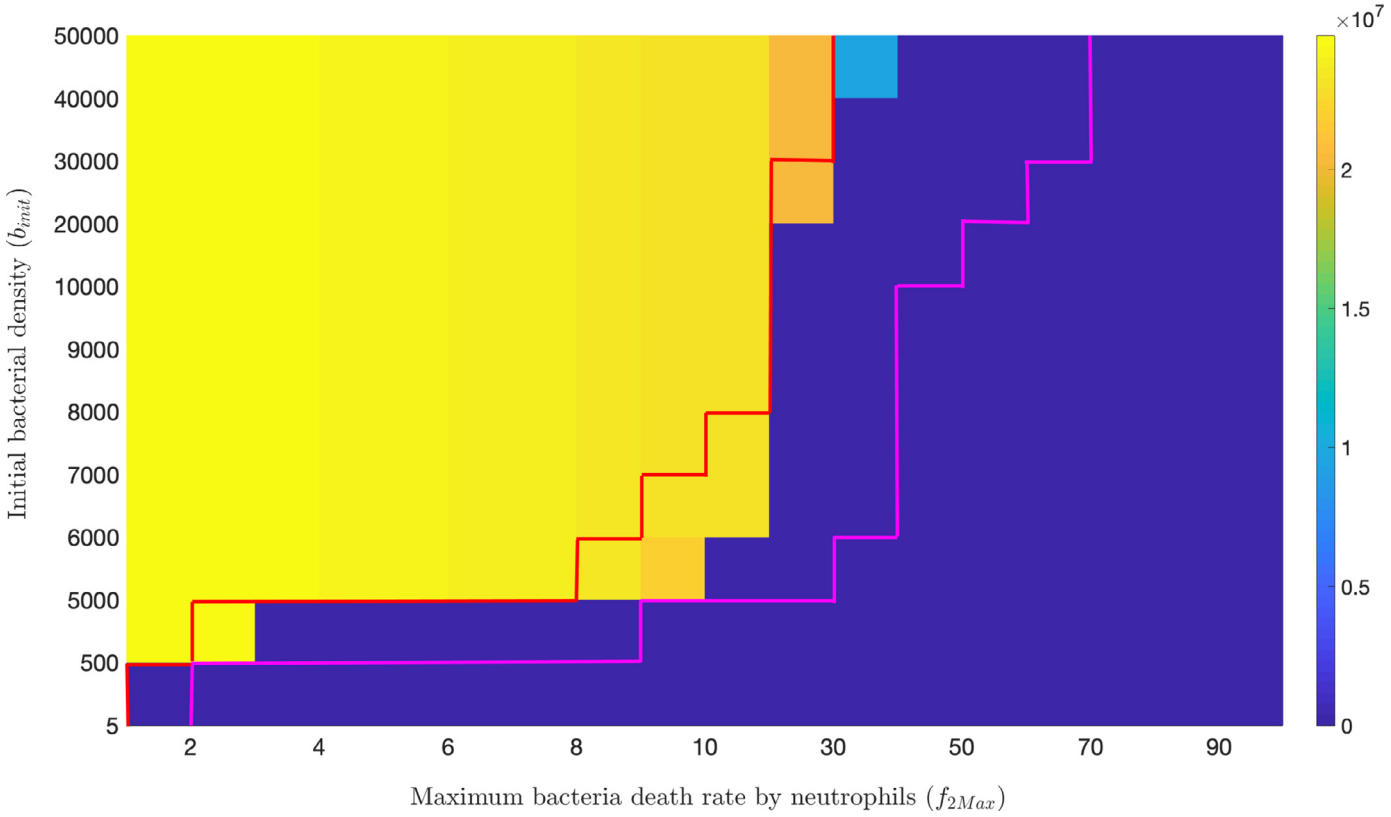

Fig. 8. Final bacterial density (at $t_{final} = 10$ days) with treatment B (80% oxygen for 6 h post surgery) as b_{init} (initial bacterial density, vertical axis) and f_{2Max} (maximum bacteria death rate by neutrophils, horizontal axis) are varied. All other parameter values are fixed as per Table 1. Surgical wounds with small initial bacterial density and/or high bacterial killing give rise to long-term bacterial elimination. For comparison, the solid red and pink lines represent the separation of the (f_{2Max}, b_{init}) parameter space in terms of bacteria elimination and bacteria infection, under no treatment (Fig. 6) and the control treatment (Fig. 7), respectively. (For interpretation of the references to colour in this figure legend, the reader is referred to the web version of this article.)

Table 2
Effect of changing each parameter by a factor of 5 (up and down), under no treatment, treatment A (30% oxygen for 2 h post surgery) and treatment B (80% oxygen for 6 h post surgery). Here, '0' represents that the surgical wound is in a state of bacteria elimination after $t_{final} = 10$ days, while '1' represents that the wound is in a state of infection after 10 days. 'N/A' refers to this parameter change being physically unrealistic, given the other baseline parameter values. Differences between results for treatment A and B are highlighted in boldfont and the parameter values for which there is a difference between treatments are listed first in the table. We note that baseline parameters in Table 1 give bacteria elimination, as shown in Fig. 4.

Parameter	No treatment ($\uparrow\times5$ / $\downarrow\times5$)	Treatment A (30%) ($\uparrow\times5$ / $\downarrow\times5$)	Treatment B (80%) ($\uparrow\times5$ / $\downarrow\times5$)
D_n	0 0	**0** 1	**1** 1
K_b	0 0	**0** 0	**1** 0
B_1	0 0	1 **0**	1 **1**
λ_9	1 0	**1** 0	**0** 0
n_0	1 1	0 1	0 1
$\overline{w}$	1 0	1 1	1 1
b_{init}	1 0	1 0	1 0
χ_n	0 1	0 1	0 1
λ_1	1 1	1 1	1 1
λ_2	1 0	1 1	1 1
D_b	0 0	0 1	0 1
W_1	1 1	0 1	0 1
W_2	1 1	1 0	1 0
f_{1Max}	1 1	1 0	1 0
f_{2Max}	0 1	0 1	0 1
D_c	1 1	1 1	1 1
λ_3	0 1	0 1	0 1
B_2	0 0	1 1	1 1
λ_4	1 0	1 1	1 1
λ_5	0 1	1 1	1 1
D_w	1 1	0 1	0 1
λ_6	0 1v	1 1	1 1
λ_7	1 1	1 1	1 1
λ_8	1 1	1 0	1 0
ε	1 1	1 1	1 1
L_1	N/A 0	N/A 0	N/A 0
L_2	0 N/A	1 N/A	1 N/A

factor of 5 (up and down) from their baseline values in Table 1; the results of this sensitivity analysis are summarised in Table 2, where '0' and '1' represent surgical wounds that are in a state of bacterial elimination and bacterial infection, respectively, after $t_{final} = 10$ days. For the baseline parameters given in Table 1 the outcome is bacteria elimination (state 0), as shown in Fig. 4. From Table 2 we can see that the experimental treatment is predicted to make no difference to the outcome after 10 days when compared to the control treatment in 93% of cases (50 of the 54 parameter sets tested), improves the outcome in 2% of cases (1 out of 54; increasing λ_9) and worsens the outcome in 5% of cases (3 out of 54; increasing D_n, increasing K_b and decreasing B_1). Increasing the oxygen supply rate (λ_9) by a factor of 5 leads to bacterial infection for the control treatment and bacterial elimination for the experimental therapy. Increasing oxygen supply will provide the neutrophils with the oxygen they need to remove the bacteria from the wound. Factors that might enable the oxygen supply to (permanently) increase include improved circulation by vascular therapy. On the other hand, increasing the carrying capacity of bacteria (K_b) or the neutrophil diffusion coefficient (D_n) by a factor of 5 gives bacteria elimination under the control treatment and bacteria infection under the experimental therapy. Increasing the carrying capacity of bacteria (K_b) allows more bacteria to occupy a given space and makes it more difficult for the neutrophils to remove the bacteria. It is possible that the carrying capacity of bacteria will depend on the local oxygen concentration, hence this may be a useful result for determining the effectiveness of oxygen treatment on SSIs. Also, reducing the bacteria density that gives half-maximal killing (B_1) by a factor of 5 gives bacteria elimination under the experimental therapy and bacteria infection under the control treatment.

Of the 50 parameter sets tested where the control and experimental treatments gave the same outcome, the no treatment case gave the same result in the majority of cases (68%; 34 out of 50), gave a better result in 10 cases (20%) and a worse outcome in 6 cases (12%). Finally, we investigated the effect of changing the location of the initial bacteria infection from the centre of the wound to a non-central location and we found no quantitative changes from bacteria elimination and infection.

4. Discussion

In this paper we have developed a simple mathematical model that simulates infection in a surgical wound by considering the interaction of neutrophils, bacteria, chemoattractant and oxygen within a domain that contains a wounded region surrounded by healthy tissue. To the best of our knowledge, this is the first mathematical model designed to assess the use of supplemental oxygen to prevent the development of clinical infection of surgical wounds. Using numerical simulations, and parameter values based on experimental literature where possible, we have found that the experimental oxygen treatment regime may be beneficial in clearing *S. aureus* bacteria from surgical sites (compare Figs. 7 and 8), however the results are dependent on the choice of model parameters (see Table 2). If parameters can be reliably estimated from appropriate data, then the model has the potential to be used as a predictive tool for testing the effect of supplemental oxygen treatments.

In 2009, Qadan et al. conducted a meta-analysis to compare the use of the control and experimental (as defined in Section 2.7) perioperative supplemental oxygen therapies to prevent the development of surgical site infections (Qadan et al., 2009). Five clinical trials were included in the meta-analysis and Qadan et al. concluded that the experimental therapy "exerts significant beneficial effect". In 2012, a meta-analysis by Togioka *et al* which combined seven clinical trials, including four of those in the Qadan et al. analysis, found that experimental oxygen therapy was not beneficial in preventing surgical site infections (Togioka et al., 2012). In 2017, Myles et al. performed a meta-analysis on 14 clinical trials, including all of the data from the Togioka *et al* study, and again concluded that there was no evidence to support the use of the experimental supplemental oxygen treatment regime to prevent surgical site infection (Myles and Kurz, 2017). It should be noted that all three meta-analyses produced results in favour of the experimental treatment, however in the two more recent studies the effect was not statistically significant. Broadly speaking, our findings are consistent with the results from the clinical trials. Firstly, our model predicts that a surgical site (regardless of treatment) can either result in establishment of a bacterial infection or bacteria elimination (Figs. 4–8). Secondly, a sensitivity analysis of our current model shows that there are parameter regimes where the experimental treatment (80% oxygen for 6 h post surgery) can have a negative impact compared to the control therapy (30% oxygen for 2 h post surgery), which is consistent with individual studies included in the meta-analyses.

Our model could be extended in several ways. In this paper, we have distinguished healthy and wound domains by the supply of neutrophils and oxygen in the healthy tissue, as well as removal of the chemoattractant. In practice, when an infection develops in healthy tissue, it can damage the tissue and extend the wound domain. Likewise, as the wound tissue heals, the wound domain will decrease in size as new blood vessels grow in response to the inflammatory signals present in the wound. We have not considered either of these factors in our mathematical model. Several mathematical models have been developed to model wound angiogenesis and repair, see for example (Flegg et al., 2012; 2010; 2009; Pettet et al., 1996), which we can leverage to extend the

current model. Furthermore, in our mathematical model, we do not consider the administration of prophylactic antibiotics that can be given to patients undergoing surgery (Hawn et al., 2013). This will play an important role in the development of an infection post surgery. One complicating factor here is that most antibiotics are oxygen-dependent (Kohanski et al., 2007; M.T. and D., 2002), so there would be an interaction between antibiotic effectiveness and oxygen levels that would need to be modelled. Other possible extensions include incorporating the supply of oxygen from below the wound and the effects of hypovolemia (state of decreased blood volume) that will alter the effectiveness of oxygen treatments (Gottrup et al., 1987).

The model could also be extended to consider surgical site infections that are co-infected with an anaerobic bacterial species, which does not need oxygen to survive. Finally, Lauffenburger and Kennedy (1981) consider several interesting cases of impaired immune response to bacteria, including defective phagocytosis (killing of bacteria by neutrophils), neutropenia (decrease in the number of circulating neutrophils) and defective emigration of neutrophils. Our model can be extended to investigate these cases (or combinations of cases) and the effect of treating them with supplemental oxygen. An indication of the effect that neutropenia and defective emigration of neutrophils exerts has been investigated here in the sensitivity analysis (see n_0 and χ_n in Table 2, respectively) where we detected no qualitative change in either case, for the range of parameters tested. A more thorough investigation could be carried out as an extension of the modelling. While these extensions might lead to more realistic models, they would also lead to more (unknown) model parameters, which need to be estimated. There is already considerable uncertainty surrounding the values of the parameters in the current model, and so it may be worthwhile obtaining more accurate estimates of these parameters before extending the model. More accurate parameter values will improve the predictive value of the current model.

With the ever-growing emphasis on the importance of sound evidence in healthcare decision-making and policy, the power of data-informed mathematical models to provide much needed insight is substantial. Here we have developed a mathematical model that can simulate the effect of supplemental oxygen therapy on a surgical site infection and give informed understanding into whether the bacteria infection is eliminated or persists.

Acknowledgements

JAF would like to acknowledge funding from the Australian Research Council (DE160100227) that supported this work.

Appendix A

Here we present an analytical solution to the spatially varying characteristic oxygen levels, w_0, that is needed in Eq. (7). We make a simplifying assumption that the oxygen concentration is dominated by degradation and neutrophil consumption. This is reasonable given that surgical wounds are created in sterile environments, with low levels of bacteria at early times. That is, we assume that the spatial distribution of oxygen is governed by the ODE:

$$0 = D_w w_0'' - \lambda_6 w_0 - \lambda_8 w_0 n_0 H(x - L_1) + \lambda_9 H(x - L_1), \tag{15}$$

subject to $w_0'(0) = w_0'(L_2) = 0$, where w_0' represents the spatial derivative of w_0. The quasi-steady state assumption is reasonable given that oxygen diffuses rapidly compared to cells (Sasaki et al., 2012); this is a common approach when modelling the interaction of chemical and cell species in the wound site (Flegg et al., 2012). Eq. (15) can be solved analytically to give an approximate expression for the oxygen distribution across the domain as input parameters (λ_6, λ_8, λ_9, D_w, n_0, L_1, L_2) vary. We can therefore analyse Eq. (7) by considering an oxygen distribution according to w_0 given by:

$$w_0(x) = \begin{cases} A\cosh\left(\sqrt{\frac{\lambda_6}{D_w}}x\right) & 0 \le x \le L_1, \\ B\cosh\left(\sqrt{\frac{\lambda_6+\lambda_8 n_0}{D_w}}(L_2 - x)\right) + \dfrac{\lambda_9}{\lambda_6+\lambda_8 n_0} & L_1 < x \le L_2, \end{cases} \tag{16}$$

where A and B are constants given by:

$$A = \frac{\frac{\lambda_9}{\sqrt{D_w(\lambda_6+\lambda_8 n_0)}}\tanh\left(\sqrt{\frac{\lambda_6+\lambda_8 n_0}{D_w}}(L_2 - L_1)\right)}{\sqrt{\frac{\lambda_6}{D_w}}\sinh\left(\sqrt{\frac{\lambda_6}{D_w}}L_1\right) + \sqrt{\frac{\lambda_6+\lambda_8 n_0}{D_w}}\tanh\left(\sqrt{\frac{\lambda_6+\lambda_8 n_0}{D_w}}(L_2 - L_1)\right)\cosh\left(\sqrt{\frac{\lambda_6}{D_w}}L_1\right)},$$

and

$$B = \frac{\frac{-\lambda_9}{\lambda_6+\lambda_8 n_0}\tanh\left(\sqrt{\frac{\lambda_6}{D_w}}L_1\right)}{\sqrt{\frac{\lambda_6}{D_w}}\cosh\left(\sqrt{\frac{\lambda_6+\lambda_8 n_0}{D_w}}(L_2 - L_1)\right)\tanh\left(\sqrt{\frac{\lambda_6}{D_w}}L_1\right) + \sqrt{\frac{\lambda_6+\lambda_8 n_0}{D_w}}\sinh\left(\sqrt{\frac{\lambda_6+\lambda_8 n_0}{D_w}}(L_2 - L_1)\right)}.$$

Supplementary material

Supplementary material associated with this article can be found, in the online version, at doi:10.1016/j.jtbi.2019.01.021.

References

Allen, D., Maguire, J., Mani, M., Wicke, C., Marcocci, L., Scheuenstuhl, H., Chang, M., Le, A., Hopf, H.W., Hunt, T.K., 1997. Wound hypoxia and acidosis limit neutrophil bacterial killing mechanisms. Arch. Surg. 132 (9), 991.

Alt, W., Lauffenburger, D., 1987. Transient behavior of a chemotaxis system modelling certain types of tissue inflammation. J. Math. Biol. 24 (6), 691–722.

Astagneau, P., Rioux, C., Golliot, F., Brucker, G., 2001. Morbidity and mortality associated with surgical site infections: results from the 1997–1999 inciso surveillance. J. Hosp. Infect. 48 (4), 267–274.

Belda, F., Aguilera, L., de la Asunción, J., Alberti, J., Vicente, R., Ferrándiz, L., Rodríguez, R., Sessler, D., Aguilar, G., Botello, S., et al., 2005. Supplemental perioperative oxygen and the risk of surgical wound infection. JAMA J. Am. Med. Assoc. 294 (16), 2035–2042.

Cheretakis, C., Leung, R., Sun, C., Dror, Y., Glogauer, M., 2006. Timing of neutrophil tissue repopulation predicts restoration of innate immune protection in a murine bone marrow transplantation model. Blood 108 (8), 2821–2826.

Chung-Sheng, S., Guey-Yueh, S., Shi-Ming, H., Yuan-Chung, K., Kuan-Lin, K., Chih-Yuan, M., Cheng-Hsiang, K., Bi-Ing, C., Chuan-Fa, C., Chun-Hung, L., et al., 2008. Lectin-like domain of thrombomodulin binds to its specific ligand lewis y antigen and neutralizes lipopolysaccharide-induced inflammatory response. Blood 112 (9), 3661–3670.

Coello, R., Charlett, A., Wilson, J., Ward, V., Pearson, A., Borriello, P., et al., 2005. Adverse impact of surgical site infections in english hospitals. J. Hosp. Infect. 60 (2), 93–103.

Davis, K.M., Mohammadi, S., Isberg, R.R., 2015. Community behavior and spatial regulation within a bacterial microcolony in deep tissue sites serves to protect against host attack. Cell Host Microbe 17 (1), 21–31.

Day, J., Rubin, J., Vodovotz, Y., Chow, C., Reynolds, A., Clermont, G., 2006. A reduced mathematical model of the acute inflammatory response ii. capturing scenarios of repeated endotoxin administration. J. Theor. Biol. 242 (1), 237–256.

Dronne, M., Boissel, J., Grenier, E., Gilquin, H., Cucherat, M., Hommel, M., Barbier, E., Bricca, G., 2004. Mathematical modelling of an ischemic stroke: an integrative approach. Acta Biotheor. 52 (4), 255–272.

Ebrahimzadeh, P., Högfors, C., Braide, M., 2000. Neutrophil chemotaxis in moving gradients of fmlp. J. Leukoc. Biol. 67 (5), 651–661.

Enoch, S., Grey, J., Harding, K., 2006. Recent advances and emerging treatments. BMJ 332, 962–965.

Flegg, J., Byrne, H., Flegg, M., McElwain, D., 2012. Wound healing angiogenesis: the clinical implications of a simple mathematical model. J. Theor. Biol. 300, 309–316.

Flegg, J., Byrne, H., McElwain, D., 2010. Mathematical model of hyperbaric oxygen therapy applied to chronic diabetic wounds. Bull. Math. Biol. 72 (7), 1867–1891.

Flegg, J., McElwain, D., Byrne, H., Turner, I., 2009. A three species model to simulate application of hyperbaric oxygen therapy to chronic wounds. PLoS Comput. Biol. 5 (7), e1000451.

Gardella, C., Goltra, L., Laschansky, E., Drolette, L., Magaret, A., Chadwick, H., Eschenbach, D., 2008. High-concentration supplemental perioperative oxygen to reduce the incidence of postcesarean surgical site infection: a randomized controlled trial. Obstet. Gynecol. 112 (3), 545–552.

Gelape, C., 2007. Surgical wound infection following heart surgery. Arq. Bras. Cardiol. 89 (1), e3–e9.

Gottrup, F., Firmin, R., Rabkin, J., Halliday, B., Hunt, T., 1987. Directly measured tissue oxygen tension and arterial oxygen tension assess tissue perfusion. Crit. Care Med. 15 (11), 1030–1036.
Greif, R., Akça, O., Horn, E., Kurz, A., Sessler, D., 2000. Supplemental perioperative oxygen to reduce the incidence of surgical-wound infection. N. Engl. J. Med. 342 (3), 161–167.
Hawn, M., Richman, J.S., Vick, C.C., Deierhoi, R.J., Graham, L.A., Henderson, W.G., Itani, K.M.F., 2013. Timing of surgical antibiotic prophylaxis and the risk of surgical site infection. JAMA Surg. 148 (7), 649–657.
Health Protection Agency (HPA), 2012. Accessed 20th June 2013.Surveillance of surgical site infections in NHS hospitals in England 2011/12. Available from: http://www.hpa.org.uk.
Hohn, D., MacKay, R., Halliday, B., Hunt, T., 1976. Effect of o2 tension on microbicidal function of leukocytes in wounds and in vitro. In: Surgical forum, 27, p. 18.
Humphreys, H., Becker, K., Dohmen, P., Petrosillo, N., Spencer, M., van Rijen, M., Wechsler-Fordos, A., Pujol, M., Dubouix, A., Garau, J., 2016. Staphylococcus aureus and surgical site infections: benefits of screening and decolonization before surgery. J. Hosp. Infect. 94, 295–304.
Hunt, T., Hopf, H., 1997. Wound healing and wound infection: what surgeons and anesthesiologists can do. Surg. Clin. N. Am. 77 (3), 587–606.
Iocono, J., Colleran, K., Remick, D., Gillespie, B., Ehrlich, H., Garner, W., 2000. Interleukin-8 levels and activity in delayed-healing human thermal wounds. Wound Repair Regen. 8 (3), 216–225.
Jeon, N., Baskaran, H., Dertinger, S., Whitesides, G., Van De Water, L., Toner, M., 2002. Neutrophil chemotaxis in linear and complex gradients of interleukin-8 formed in a microfabricated device. Nat. Biotechnol. 20 (8), 826–830.
Kim, J., Pitts, B., Stewart, P., Camper, A., Yoon, J., 2008. Comparison of the antimicrobial effects of chlorine, silver ion, and tobramycin on biofilm. Antimicrob. Agents Chemother. 52 (4), 1446–1453.
Kohanski, M., Dwyer, D., Hayete, B., Lawrence, C., Collins, J., 2007. A common mechanism of cellular death induced by bactericidal antibiotics. Cell 130, 797–810.
Laterveer, L., Lindley, I., Heemskerk, D., Camps, J., Pauwels, E., Willemze, R., Fibbe, W., 1996. Rapid mobilization of hematopoietic progenitor cells in rhesus monkeys by a single intravenous injection of interleukin-8. Blood 87 (2), 781–788.
Lauffenburger, D., 1983. Measurement of phenomenological parameters for leukocytemotility and chemotaxis. Agents Actions Suppl. 12, 34–53.
Lauffenburger, D., Kennedy, C., 1981. Analysis of a lumped model for tissue inflammation dynamics. Math. Biosci. 53, 189–221.
Lauffenburger, D., Kennedy, C., 1983. Localized bacterial infection in a distributed model for tissue inflammation. J. Math. Biol. 16 (2), 141–163.
Maggelakis, S., 2003. A mathematical model of tissue replacement during epidermal wound healing. Appl. Math. Model. 27 (3), 189–196.
MathWorks, 15 November 2017. PDEPE Manual. https://au.mathworks.com/help/matlab/ref/pdepe.html.
Mayzler, O., Weksler, N., Domchik, S., Klein, M., Mizrahi, S., Gurman, G., et al., 2005. Does supplemental perioperative oxygen administration reduce the incidence of wound infection in elective colorectal surgery. Minerva Anestesiol. 71 (1–2), 21–25.
Mi, Q., Rivière, B., Clermont, G., Steed, D., Vodovotz, Y., 2007. Agent-based model of inflammation and wound healing: insights into diabetic foot ulcer pathology and the role of transforming growth factor-β1. Wound Repair Regen. 15 (5), 671–682.
Min-Ho, K., Wei, L., Borjesson, D., Curry, F., Miller, L., Cheung, A., Fu-Tong, L., Isseroff, R., Simon, S., 2008. Dynamics of neutrophil infiltration during cutaneous wound healing and infection using fluorescence imaging. J. Invest. Dermatol. 128 (7), 1812–1820.
Moghe, P., Nelson, R., Tranquillo, R., 1995. Cytokine-stimulated chemotaxis of human neutrophils in a 3-d conjoined fibrin gel assay. J. Immunol. Methods 180 (2), 193–211.
M.T., S., D., L., 2002. The antibacterial activity of vancomycin towards staphylococcus aureus under aerobic and anaerobic conditions. J. Appl. Microbiol. 92, 866–872.
Myles, P.S., Kurz, A., 2017. Supplemental oxygen and surgical site infection: getting to the truth. BJA: Br. J. Anaesth. 119 (1), 13–15. doi:10.1093/bja/aex096.
Pettet, G., Byrne, H., McElwain, D., Norbury, J., 1996. A model of wound-healing angiogenesis in soft tissue. Math. Biosci. 136 (1), 35–63.
Qadan, M., Akca, O., Mahid, S., Hornung, C., Polk Jr, H., 2009. Perioperative supplemental oxygen therapy and surgical site infection: a meta-analysis of randomized controlled trials. Arch. Surg. 144 (4), 359.
Reynolds, A., Rubin, J., Clermont, G., Day, J., Vodovotz, Y., Bard Ermentrout, G., 2006. A reduced mathematical model of the acute inflammatory response: i. derivation of model and analysis of anti-inflammation. J. Theor. Biol. 242 (1), 220–236.
Romanyukha, A., Rudnev, S., Sidorov, I., 2006. Energy cost of infection burden: an approach to understanding the dynamics of host–pathogen interactions. J. Theor. Biol. 241 (1), 1–13.
Rudnev, S., Romanyukha, A., 1995. Mathematical modeling of immune-inflammatory reaction in acute pneumonia. J. Biol. Syst. 3 (02), 429–439.
Sasaki, N., Horinouchi, H., Ushiyama, A., Minamitani, H., 2012. A new method for measuring the oxygen diffusion constant and oxygen consumption rate of arteriolar walls. Keio J Med 61 (2), 57–65.
Schugart, R., Friedman, A., Zhao, R., Sen, C., 2008. Wound angiogenesis as a function of tissue oxygen tension: a mathematical model. Proc. Nat. Acad. Sci. 105 (7), 2628–2633.
Shen, L., Smith, J.M., Shen, Z., Hussey, S.B., Wira, C.R., Fanger, M.W., 2006. Differential regulation of neutrophil chemotaxis to il-8 and fmlp by gm-csf: lack of direct effect of oestradiol. Immunology 117 (2), 205–212.
Sherratt, J., Chaplain, M., 2001. A new mathematical model for avascular tumour growth. J. Math. Biol. 43 (2), 291–312.
Singer, M., Sansonetti, P.J., 2004. Il-8 is a key chemokine regulating neutrophil recruitment in a new mouse model of shigella-induced colitis. J. Immunol. 173 (6), 4197–4206.
Smith, A., McCullers, J., Adler, F., 2011. Mathematical model of a three-stage innate immune response to a pneumococcal lung infection. J. Theor. Biol. 276 (1), 106–116.
Stephen, W., 2013. In: Jacob, B. (Ed.), The method of volume averaging. Springer Science & Business Media, Technion - Israel Institute of Technology, Haifa, Israel.
Stokes, C., D.A., L., 1991. Analysis of the roles of microvessel endothelial cell random motility and chemotaxis in angiogenesis. J Theor Biol 152, 377–403.
Togioka, B., Galvagno, S., Sumida, S., Murphy, J., Ouanes, J., Wu, C., 2012. The role of perioperative high inspired oxygen therapy in reducing surgical site infection: a meta-analysis. Anesth. Analg. 114 (2), 334–342.
Vermolen, F., Adam, J., 2007. A Finite Element Model for Epidermal Wound Healing. In: Computational Science–ICCS 2007. Springer, pp. 70–77.
Wood, B., Quintard, M., Whitaker, S., 2002. Calculation of effective diffusivities for biofilms and tissues. Biotechnol. Bioeng. 77 (5), 495–516.
Yeong-Chul, K., 1996. Diffusivity of bacteria. Korean J. Chem. Eng. 13 (3), 282–287.
Zimlichman, E., Henderson, D., Tamir, O., Franz, C., Song, P., Yamin, C.K., Keohane, C., Denham, C.R., Bates, D.W., 2013. Health care–associated infections: a meta-analysis of costs and financial impact on the us health care system. JAMA Intern Med 173 (22), 2039–2046.
Zwietering, M.H., Jongenburger, I., Rombouts, F.M., van't Riet, K., 1990. Modeling of the bacterial growth curve. Appl. Environ. Microbiol. 1875–1881.